pyridine rings of one phenanthroline subunit are respectively 8 (1)° with N3 and N4 involved and 10.54 (8)° with N1 and N2. The preference of cobalt for an octahedral geometry is such that the constraint imposed by the CH_2CH_2 bridges leads to a distortion of the phenanthroline subunit. This may also be the reason for the lack of double-helix formation.

When ligand 3 was treated with iron(II) salts, a 3:2 ligand/metal complex **3a** (m/z 1509.1, $[M - ClO_4]^+$) with a deep red color characteristic of a "Fe(bpy)$_3$" species (Table II), was quantitatively isolated. The structure of complex **3a** might be close to that recently described for an analogous triply bridged dinuclear iron species consisting of three bridging 1,2-bis(4'-methyl-2,2'-bipyridin-4-yl)ethane ligands linking the two Fe(II) centers.[4] The dinuclear iron complex $[Fe_2(3)_3](ClO_4)_4$ was oxidized by cyclic voltammetry in a single reversible dielectronic wave at $E_{1/2}$ = +0.88 V, which compares well with its $[Fe(bpy)_3[(ClO_4)_2$ analogue value of $E_{1/2}$ = +0.70 V.[29]

Conclusion

The present results show that ligands containing two bipyridine or two phenanthroline groups linked by a CH_2CH_2 bridge are able to form a double-stranded helicate by complexation with copper(I). In the case of cobalt(II), the strong tendency to form an octahedral geometry prevents the formation of such a helix.

The double-helical structure of the dinuclear copper complexes was assigned by NMR spectroscopy for **1a** and **2a** and confirmed by the X-ray structure analysis for **1a**. Twisting forces the proton α to the ethane bridge to be in the shielding region of the bipyridine or phenanthroline subunit of the second ligand, a feature characteristic of the existence of a double helix in a given compound.

Finally, the dinuclear copper and iron complexes are oxidized in a single reversible dielectronic wave; this seems to indicate that each redox center is almost electronically independent. Related conjugated ligands might give access to coupled redox centers (see also ref 6).

Acknowledgment. We thank Patrick Maltèse for determining the NOE-DIFF NMR spectra and the CNRS for financial support.

Registry No. **1**, 120096-05-1; **1a**, 132298-91-0; **2**, 120096-06-2; **2a**, 132298-93-2; **2b**, 132298-94-3; **3a**, 132343-37-4; $[Cu_2(\mathbf{1})_2]^{3+}$, 132298-96-5; $[Cu_2(\mathbf{2})_2]^{3+}$, 132298-97-6; $[Co(\mathbf{2})](CF_3SO_3)_2^-$, 132298-98-7; $[Co(\mathbf{2})](CF_3SO_3)_2^{2-}$, 132343-38-5; $[Co(\mathbf{2})](CF_3SO_3)_2^{3-}$, 132298-99-8; $[Fe_2(\mathbf{3})_3]^{5+}$, 132299-00-4; $[Cu(CH_3CN)_4](ClO_4)$, 14057-91-1; $[Co(DMSO)_6](CF_3SO_3)_2$, 132298-95-4; $[Cu(dmbpy)_2]^{2+}$, 90316-91-9; $[Cu_2(p\text{-}QP)_2]^{3+}$, 97093-39-5; $[Cu_2(p\text{-}QP)_2]^{4+}$, 132299-01-5; $[Cu(dmphen)_2]^{2+}$, 14875-91-3; $[Co(bpy)_3]^{3+}$, 19052-39-2; $[Co(bpy)_3]^+$, 47780-35-8; $[Co(bpy)_3]$, 29931-78-0; $[Fe(bpy)_3]^{3+}$, 18661-69-3; $[Cu(dmbpy)_2](CF_3SO_3)$, 116184-54-4; $[Cu_2(p\text{-}QP)_2](ClO_4)_2$, 88178-45-4; $[Cu(dmphen)_2](CF_3COO)$, 132299-02-6; $[Co(bpy)_3](ClO_4)_2$, 21349-81-5; $[Fe(bpy)_3](ClO_4)_2$, 15388-48-4.

Supplementary Material Available: Tables of positional parameters and isotropic thermal parameters, bond lengths, bond angles, anisotropic thermal parameters, and hydrogen atom parameters (21 pages); tables of observed and calculated structure factors (28 pages). Ordering information is given on any current masthead page.

---

(29) Brandt, W. W.; Dwyer, F. P.; Gyarfas, E. C. *Chem. Rev.* **1954**, *54*, 959.

Contribution from the Lehrstuhl für Anorganische Chemie I, Ruhr-Universität, D-4630 Bochum, FRG,
Institut für Physikalische Chemie, Technische Hochschule, D-6100 Darmstadt, FRG, Institut für Physik,
Medizinische Universität, D-2400 Lübeck, FRG, and Anorganisch-Chemisches Institut der Universität, D-6900 Heidelberg, FRG

Syntheses, Redox Behavior, and Magnetic and Spectroscopic Properties of $Cu^{II}Cu^{II}Cu^{II}$, $Cu^{II}Ni^{II}Cu^{II}$, and $Cu^{II}Pd^{II}Cu^{II}$ Species. Crystal Structure of $[L_2Cu_2Cu(dmg)_2Br]ClO_4\cdot CH_3OH$ (L = 1,4,7-Trimethyl-1,4,7-triazacyclononane; dmg = Dimethylglyoximato(2–))

Phalguni Chaudhuri,[*,†] Manuela Winter,[†] Beatriz P. C. Della Védova,[†] Eckhard Bill,[‡] Alfred Trautwein,[‡]
Stefan Gehring,[§] Peter Fleischhauer,[§] Bernhard Nuber,[‖] and Johannes Weiss[‖]

Received July 18, 1990

A series of homo- and heterotrinuclear complexes $Cu^{II}Cu^{II}Cu^{II}$, $Cu^{II}Ni^{II}Cu^{II}$, and $Cu^{II}Pd^{II}Cu^{II}$ containing the dimethylglyoximato dianion as bridging ligands and either 1,4,7-trimethyl-1,4,7-triazacyclononane or *N,N,N',N'*-tetramethylethylenediamine as capping ligands have been synthesized and characterized on the basis of IR, electronic, and EPR spectroscopy and variable-temperature (4–290 K) magnetic susceptibility measurements. The crystal and molecular structure of the compound $[L_2Cu_2(dmg)_2CuBr]ClO_4\cdot CH_3OH$ has been established by X-ray diffraction. It crystallizes in orthorhombic system, space group *Pnam* with lattice constants a = 14.006 (7) Å, b = 15.972 (8) Å, c = 19.27 (1) Å, and Z = 4. The structure consists of $Cu^{II}Cu^{II}Cu^{II}$ trinuclear cations, uncoordinated perchlorate anions, and a methanol molecule of crystallization. Each copper ion is in a square-pyramidal environment. The $Cu(dmg)_2^{2-}$ dianion functions as a bridge between two terminal copper ions through its deprotonated oximate oxygen and represents the central copper atom in the trinuclear unit. The central copper atom is coordinated also to a bromide ion. The terminal copper ions achieve a CuN_3O_2 chromophore structure by coordinating to three nitrogen atoms of the cyclic amine and the deprotonated oxygen atoms of dimethylglyoxime dianion. A strong antiferromagnetic interaction ($J = -448\ cm^{-1}$) between adjacent Cu(II) ions has been found for the aforementioned compound, showing that dimethylglyoxime is a good mediator for spin-exchange interactions. A moderately strong antiferromagnetic interaction ($2J = -72\ cm^{-1}$) has been observed for a $Cu^{II}Pd^{II}Cu^{II}$ system, with a diamagnetic square-planar Pd(II) as the central ion, although the Cu···Cu separation is expected to be ca. 7.6 Å. The powder EPR spectra indicate square-pyramidal geometry for the copper with a $(d_{x^2-y^2})^1$ ground state in the homotrinuclear complexes. EPR spectra of heterotrinuclear complexes are quasi-isotropic. The cyclic voltammograms of the $Cu^{II}Cu^{II}Cu^{II}$ complexes revealed, besides other features, a quasi-reversible one-electron oxidation corresponding to the reversible formation of the mixed-valence species $Cu^{II}Cu^{III}Cu^{II}$.

Introduction

Current research work concerning the structural and magnetic properties of polynuclear transition-metal compounds is aimed at understanding the structural and chemical features governing electronic exchange coupling through multiatom bridging ligands.[1-3] This problem has important implications for topics such

---

[†] Ruhr-Universität Bochum.

[‡] Medizinische Universität Lübeck.

[§] Technische Hochschule Darmstadt.

[‖] Universität Heidelberg.

(1) Hendrickson, D. N. In *Magneto-Structural Correlations in Exchange Coupled Systems*; Willett, R. D., Gatteschi, D., Kahn, O., Eds.; NATO ASI Series C; Mathematical and Physical Science; Reidel: Dordrecht, The Netherlands, 1985; p 523.

as the nature of orbital interactions, electron transfer in redox reaction precursors, and biological electron-transport chains. The system is of further interest for the study of long-range magnetic interactions with its underlying biological importance. The literature on this subject is exhaustive,[4,5] mainly dealing with dimeric compounds and chains. Although the greatest effort and success have been in the study of dinuclear copper(II) complexes, there has been relatively little work on oligomeric copper(II) complexes with more than two copper ions, particularly on linear trinuclear compounds,[6-12] primarily due to a lack of suitably characterized compounds.

The reported trinuclear copper(II) complexes exhibit varying degrees of exchange interaction, both antiferromagnetic and ferromagnetic. The molecular structures of these complexes have revealed mainly three kinds of trinuclear copper clusters, consisting of triangular arrays (isosceles I or equilateral II) of copper ions

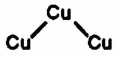

C_{2v}, I

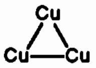

D_{3h}, II

$D_{\infty h}$, III

and of strict linearly (III) arranged copper ions. A fourth type, a μ_3-carbonato-bridged trinuclear copper cluster with a spin-triplet ground state, has also been reported.[13]

A trinuclear copper cluster may be of importance in a number of the multicopper blue oxidases,[14] such as ascorbate oxidase and laccase. These multicopper blue oxidases catalyze the four-electron reduction of oxygen to water with concomitant one-electron oxidation of a variety of substrates, such as ascorbate, polyphenols, and aromatic polyamines. A recent X-ray structure[15] determination at 2.5-Å resolution on oxidized ascorbate oxidase from zucchini unambiguously demonstrated the existence of a 3 + 1 arrangement of the copper atoms. Such a 3 + 1 structure has recently also been considered[14] as a possibility for the manganese cluster of the water oxidation center (which catalyzes the reverse reaction of ascorbate oxidase) in the photosystem II of plants.

Our continuing interest in copper chemistry[16] led us to study new trinuclear copper(II) complexes with the small tridentate cyclic amine 1,4,7-trimethyl-1,4,7-triazacyclononane (L).[17] This ligand coordinates facially with one nitrogen in the apical position and prevents for steric reasons the formation of ML_2 moieties; only one ligand per metal center can be bound.[18] This ligand prefers to impose a square-based pyramidal geometry around copper(II) ions and hence a $(d_{x^2-y^2})^1$ ground state. We have also used tetramethylethylenediamine (L′) as the capping ligand, which imposes either a square-planar or square-based pyramidal geometry around the terminal copper(II) ions, in order to make a comparison between L and L′.

The paucity of bis(oximato)metal(II) groups as bridging ligands in coordination chemistry is surprising.[19] With the aim of providing some answers to questions regarding the effectiveness of polyatomic bridging ligands like oximes and their metal complexes in propagating exchange interaction, we have prepared the following homo- and heterotrinuclear complexes containing $[M^{II}(\text{dimethylglyoximato})_2]^{2-}$ (M = Cu, Ni, Pd) as bridging ligands.

homotrinuclear complexes	
$[L_2Cu_2Cu(dmg)_2](ClO_4)_2$	**1**
$[L_2Cu_2Cu(dmg)_2Br]ClO_4\cdot CH_3OH$	**4**
$[L'_2Cu_2(OH_2)_2Cu(dmg)_2](ClO_4)_2$	**6**
heterotrinuclear complexes	
$[L_2Cu_2Ni(dmg)_2(OH_2)_2](ClO_4)_2$	**2**
$[L_2Cu_2Pd(dmg)_2](ClO_4)_2\cdot 2H_2O$	**3**
$[L_2Cu_2Ni(dmg)_2Br(OH_2)]PF_6\cdot H_2O$	**5**
$[L'_2Cu_2(OH_2)_2Pd(dmg)_2](ClO_4)_2$	**7**

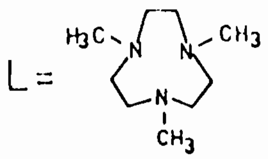

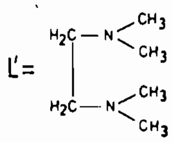

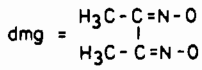
$$\text{dmg} = \begin{array}{l} H_3C-C{=}N-O^{\ominus} \\ \quad\;\;\; | \\ H_3C-C{=}N-O^{\ominus} \end{array}$$

We describe here the characterization of these complexes by electrochemistry, by magnetic susceptometry and by IR, EPR, and UV/vis spectroscopies. The crystal structure of the compound $[L_2Cu_2Cu(dmg)_2Br]ClO_4\cdot CH_3OH$ (**4**) is also included. Throughout this paper, the trinuclear complexes are denoted by the respective metal centers only; the terminal and bridging ligands are omitted for simplicity.

Experimental Section

Materials and Methods. The macrocycle 1,4,7-trimethyl-1,4,7-triazacyclononane was prepared as previously described.[17] All other starting materials were commercially available and of reagent grade. Elemental microanalyses (C, H, N) were performed by the Microanalytical Laboratory, Ruhr-Universität Bochum. Copper was determined gravimetrically by using *N*-benzoyl-*N*-phenylhydroxylamine. The perchlorate anion was determined gravimetrically as tetraphenylarsonium(V) perchlorate. Electronic absorption spectra were measured on a Perkin-Elmer Lambda 9 spectrophotometer in solution with methanol or acetonitrile used as solvent. The positions of the absorption maxima were checked by measuring the reflectance spectra (KBr disks) of the respective solid in order to ensure the identity of the species in solution and in the solid state. Fourier transform infrared spectroscopy on KBr pellets was performed on a Perkin-Elmer 1720X FT-IR instrument.

Magnetic susceptibilities of powdered samples were recorded on a Faraday-type magnetometer using a sensitive Cahn RG electrobalance in the temperature range 4.2–289.5 K. The applied magnetic field was ≈1.2 T. Details of the apparatus have already been described elsewhere.[20] Experimental susceptibility data were corrected for the underlying diamagnetism. Corrections for diamagnetism were estimated as -479×10^{-6}, -500×10^{-6}, -488×10^{-6}, -464×10^{-6}, -522×10^{-6}, -422×10^{-6} and -436×10^{-6} cm^3/mol for complexes **1**–**7**, respectively.

---

(2) Hatfield, W. E. In *Theory and Applications of Molecular Paramagnetism*; Boudreaux, E. A., Mulay, L. N., Eds.; John Wiley & Sons: New York, 1976; p 350.

(3) Sinn, E. *Coord. Chem. Rev.* **1970**, *5*, 313.

(4) Kahn, O. *Angew. Chem.* **1985**, *97*, 837.

(5) (a) Willett, R. D. In *Magneto-Structural Correlations in Exchange Coupled Systems*; Willett, R. D., Gatteschi, D., Kahn, O., Eds.; Reidel: Dordrecht, The Netherlands, 1985; p 348. (b) Hatfield, W. E. *Ibid.*; p 555.

(6) Ginsberg, A. P.; Martin, R. L.; Sherwood, R. C. *Inorg. Chem.* **1968**, *7*, 932.

(7) Brown, D. V.; Wasson, J. R.; Hall, J. W.; Hatfield, W. E. *Inorg. Chem.* **1977**, *16*, 2526.

(8) Vos, V.; de Graaff, R. A. G.; Haasnoot, J. G.; van der Kraan, A. M.; de Vaal, P.; Reedijk, J. *Inorg. Chem.* **1984**, *23*, 2905.

(9) Haase, W.; Gehring, S. *J. Chem. Soc., Dalton Trans.* **1985**, 2609 and references therein.

(10) Journaux, Y.; Sletten, J.; Kahn, O. *Inorg. Chem.* **1986**, *25*, 439 and references therein.

(11) Luneau, D.; Oshio, O.; Okawa, H.; Kida, S. *Chem. Lett.* **1989**, 443.

(12) Baker, W. A.; Helm, F. T. *J. Am. Chem. Soc.* **1975**, *97*, 2295 and references therein.

(13) Kolks, G.; Lippard, S. J.; Waszczak, J. V. *J. Am. Chem. Soc.* **1980**, *102*, 4832.

(14) Huber, R. *Angew. Chem.* **1989**, *101*, 849.

(15) Messerschmidt, A.; Rossi, A.; Ladenstein, R.; Huber, R.; Bolognesi, M.; Gatti, G.; Marchesini, A.; Petruzzelli, R.; Finazzi-Agro, A. *J. Mol. Biol.* **1989**, *206*, 513.

(16) (a) Chaudhuri, P.; Oder, K. *J. Chem. Soc., Dalton Trans.* **1990**, 1597. (b) Chaudhuri, P., Oder, K. *J. Organomet. Chem.* **1989**, *367*, 249. (c) Chaudhuri, P.; Ventur, D.; Wieghardt, K.; Peters, E. M.; Peters, K.; Simon, A. *Angew. Chem., Int. Ed. Engl.* **1985**, *24*, 57. (d) Chaudhuri, P.; Wieghardt, K.; Nuber, B.; Weiss, J. *J. Chem. Soc., Chem. Commun.* **1985**, 265. (e) Chaudhuri, P.; Oder, K.; Wieghardt, K.; Nuber, B.; Weiss, J. *Inorg. Chem.* **1986**, *25*, 2818. (f) Chaudhuri, P.; Oder, K.; Wieghardt, K.; Gehring, S.; Haase, W.; Nuber, B.; Weiss, J. *J. Am. Chem. Soc.* **1988**, *110*, 3657.

(17) Wieghardt, K.; Chaudhuri, P.; Nuber, B.; Weiss, J. *Inorg. Chem.* **1982**, *21*, 3086.

(18) Chaudhuri, P.; Wieghardt, K. *Prog. Inorg. Chem.* **1987**, *35*, 330.

(19) During the preparation of the present paper a paper describing the bis(dimethylglyoximato)cuprate(II) group as a bridging ligand has been published: Okawa, H.; Koikawa, M.; Kida, S.; Luneau, D.; Oshio, H. *J. Chem. Soc., Dalton Trans.* **1990**, 469.

(20) Merz, L.; Haase, W. *J. Chem. Soc., Dalton Trans.* **1980**, 875.

The TIP values were considered to be 60 × 10^{-6} cm^3/mol of Cu.

The polycrystalline X-band EPR spectra were recorded at various temperatures between 4.2 and 300 K with a Bruker 200 spectrometer equipped with a helium continuous-flow cryostat, a NMR gaussmeter, a frequency meter, and a data acquisition system (our own development).

Cyclic voltammetry experiments were performed with a Princeton Applied Research Model 173 potentiostat–galvanostat driven by a Model 175 universal programmer. Voltammograms were recorded on a Kipp & Zonen XY recorder, Model BD 90. Fast voltammograms (≥1 V s^{-1}) were recorded on a Gould OS 4200 digital storage oscilloscope. The supporting electrolyte was 0.1 M $NBu^n_4PF_6$ in methylene chloride or acetonitrile. A standard three-electrode cell was employed with a glassy-carbon working electrode, a platinum-wire auxilliary electrode, and a silver/silver chloride (saturated LiCl in ethanol) reference electrode. Measurements were made under an argon atmosphere at 25 °C. At the beginning of each experiment, a cyclic voltammogram of the solution containing only the supporting electrolyte was measured. To this solution, solid samples of trinuclear complexes were added and dissolved under stirring to achieve a concentration of $\approx 10^{-3}$ M of the electroactive component. The potential of the reference electrode was determined to be ≈–0.06 V vs NHE by using the Fc^+/Fc couple as the internal standard.

Preparation of Compounds. $M(C_4N_2H_7O_2)_2$ (M^{II} = Cu, Ni, Pd). These bis(dimethylglyoximato)metal(II) compounds were prepared by addition of a sample of $M(CH_3COO)_2 \cdot xH_2O$ to an ammoniacal solution of dimethylglyoxime in ethanol in an appropriate ratio.

$[(C_9H_{21}N_3)_2Cu_2M(C_4N_2H_6O_2)_2](ClO_4)_2 \cdot xH_2O$ (M^{II} = Cu (1), Ni (2), Pd (3)). Because all these complexes were prepared in a very similar way, a representative method only is described. A solution of the cyclic amine (0.34 g, 2 mmol) in 60 mL of methanol was treated with a sample of $Cu(ClO_4)_2 \cdot 6H_2O$ (0.74 g, 2 mmol) under vigorous stirring in a round-bottomed flask. After 0.25 h of stirring, the blue solution was charged with a sample of $M(C_4N_2H_7O_2)_2$ (1 mmol) and 1 mL (for **1**) or 3 mL (for **2** and **3**) of triethylamine. The resulting suspension was refluxed for 0.5 h to obtain a clear solution. The dark colored solution was filtered to get rid of any solid particles, followed by an addition of 0.6 g of $NaClO_4 \cdot H_2O$ to the filtrate. The solution kept at ambient temperature provided deep brown (almost black) crystals for the Cu_2Cu and Cu_2Ni complexes and deep green crystals for the Cu_2Pd complex. The crystals were collected by filtration and air-dried. Yield: 60–80%.

Anal. Calcd for $Cu_3C_{26}H_{54}N_{10}O_{12}Cl_2$ (**1**): C, 32.52; H, 5.67; N, 14.58; Cu, 19.58; ClO_4, 20.71. Found: C, 32.32; H, 5.58; N, 14.43; Cu, 20.3; ClO_4, 20.4.

Anal. Calcd for $Cu_2NiC_{26}H_{54}N_{10}O_{12}Cl_2 \cdot 2H_2O$ (**2**): C, 31.50; H, 5.70; N, 14.13; Cu, 12.82; Ni, 5.92; ClO_4, 20.06. Found: C, 31.6; H, 5.8; N, 14.1; Cu, 12.6; Ni, 5.8; ClO_4, 19.7.

Anal. Calcd for $Cu_2PdC_{26}H_{54}N_{10}O_{12}Cl_2$ (**3**): C, 31.07; H, 5.62; N, 13.94; Cu, 12.64; ClO_4, 19.79. Found: C, 30.9; H, 5.60; N, 13.90; Cu, 12.5; ClO_4, 19.6.

$[(C_9H_{21}N_3)_2Cu_2Cu(C_4N_2H_6O_2)_2Br]ClO_4 \cdot CH_3OH$ (4). Complex **4** was obtained in a similar way as for **1** by using anhydrous $CuBr_2$ instead of $Cu(ClO_4) \cdot 6H_2O$ as the copper source as deep brown crystals. Yield: ≈65%.

Anal. Calcd for $Cu_3C_{27}H_{58}N_{10}O_9BrCl$: C, 33.33; H, 6.01; N, 14.40; Cu, 19.60; ClO_4, 10.22. Found: C, 33.1; H, 5.92; N, 14.4; Cu, 19.8; ClO_4, 10.1.

$[(C_9H_{21}N_3)_2Cu_2Ni(C_4N_2H_6O_2)_2]Br(PF_6) \cdot 2H_2O$ (5). Complex **5** was obtained analogously by using $CuBr_2$, $Ni(C_4N_2H_7O_2)_2$, triethylamine, and $NaPF_6$ as the counterion supplier as deep brown-green crystals. Yield: 70%.

Anal. Calcd for $Cu_2NiC_{26}H_{58}N_{10}O_6BrPF_6$: C, 30.69; H, 5.75; N, 13.77; Cu, 12.49. Found: C, 30.62; H, 5.90; N, 13.70; Cu, 12.60.

$[(C_6H_{16}N_2)_2Cu_2(OH_2)_2M(C_4H_6N_2O_2)_2](ClO_4)_2$ (M = Cu(II) (6), Pd(II) (7)). Complexes **6** and **7** were obtained as brown and green crystals, respectively, in a similar way as for **1** and **3** by using *N,N,N',N'*-tetramethylethylenediamine (L′) instead of the cyclic amine (L). Yield: 80% for **6**; 65% for **7**.

Anal. Calcd for $Cu_3C_{20}H_{48}N_8O_{14}Cl_2$ (**6**): C, 27.11; H, 5.46; N, 12.64; Cu, 21.51; ClO_4, 22.44. Found: C, 27.2; H, 5.4; N, 12.70; Cu, 21.8; ClO_4, 22.2.

Anal. Calcd for $Cu_2PdC_{20}H_{48}N_8O_{14}Cl_2$ (**7**): C, 25.86; H, 5.21; N, 12.06; Cu, 13.68; ClO_4, 21.41. Found: C, 25.9; H, 5.3; N, 12.1; Cu, 13.5; ClO_4, 21.5. Complexes **1**–**7** were recrystallized from methanol or acetonitrile in the presence of triethylamine, in case $M(dmgH)_2$ was present as impurities in the obtained trinuclear complexes.

Caution! Although we experienced no difficulties with the compounds isolated as their perchlorate salts, the unpredictable behavior of perchlorate salts necessitates extreme caution in their handling.

Crystal Structure Determinations. A dark brown (almost black) prismatic crystal of $Cu_3(C_9H_{21}N_3)_2(C_4N_2H_6O_2)_2Br(ClO_4) \cdot CH_3OH$ with dimensions of 0.27 × 0.49 × 0.76 mm was mounted on a Siemens AED II four-circle diffractometer. Preliminary examinations showed that the crystal belonged to the orthorhombic crystal system, space group $D_{2h}{}^{16}$-*Pnam*. The unit cell parameters were obtained at 23 °C by a least-square refinement of the angular settings (8° < 2θ < 29°) of 25 reflections. The data are summarized in Table I along with details of the treatment of the intensity data. The data were corrected for Lorentz and polarization effects, but it was unnecessary to account for crystal decay. An empirical absorption correction[21] was carried out (ψ scans). The scattering factors[22] for neutral non-hydrogen atoms were corrected for both the real and the imaginary components of anomalous dispersion. The structure was solved by conventional Patterson and Fourier-difference syntheses. The structure was refined by least-squares techniques; the function minimized was $\sum w(|F_o| - |F_c|)^2$ where $w = 1/\sigma^2(I)$. Idealized positions of H atoms bound to carbon atoms were calculated and included in the refinement cycles with a common isotropic thermal parameter (U = 0.080 $Å^2$). All other atoms were refined anisotropically. The methanol molecule of the crystal was found to be disordered and was refined as two carbon atoms (C(21) and C(22)). Refinement considering a carbon and an oxygen atom did not change the situation. Perchlorate anion was found to be disordered and was refined isotropically. Final positional parameters for all non-hydrogen atoms are given in Table II.

Table I. Crystallographic Data for $[L_2Cu_2(dmg)_2CuBr]ClO_4 \cdot CH_3OH$

formula	$Cu_3C_{27}H_{58}N_{10}O_9BrCl$	Z	4
fw	972.83	ρ_{calcd}/g cm^{-3}	1.49
space group	*Pnam* (No. 62)	μ(Mo Kα)/mm^{-1}	2.19
a/Å	14.006 (7)	R	0.083
b/Å	15.972 (8)	R_w	0.069
c/Å	19.27 (1)	T/°C	22
V/Å	4311 (6)	λ/Å (Mo Kα, graphite monochromated)	0.71069

Table II. Atomic Coordinates (×10^4) for $[L_2Cu_2(dmg)_2CuBr]ClO_4 \cdot CH_3OH$

atom	x	y	z
Cu(1)	1394 (2)	2500	5671 (1)
Cu(2)	1859 (2)	446 (1)	5920 (1)
Br(1)	2856 (2)	2500	6478 (2)
N(4)	564 (9)	1708 (7)	6167 (7)
N(5)	1744 (9)	1704 (7)	4941 (6)
O(1)	637 (7)	876 (5)	6171 (5)
O(2)	1784 (8)	852 (6)	4989 (5)
N(1)	3249 (12)	72 (9)	5777 (11)
N(2)	1569 (13)	–903 (8)	5654 (10)
N(3)	2091 (14)	33 (10)	6931 (9)
C(1)	3286 (16)	–715 (14)	5464 (15)
C(2)	2437 (17)	–1077 (14)	5239 (14)
C(3)	1451 (16)	–1256 (12)	6363 (13)
C(4)	1540 (20)	–719 (16)	6949 (10)
C(5)	3118 (18)	–156 (14)	6972 (13)
C(6)	3710 (18)	154 (17)	6447 (15)
C(7)	3816 (13)	618 (11)	5340 (11)
C(8)	686 (13)	–1028 (10)	5301 (10)
C(9)	1729 (4)	606 (10)	7474 (9)
C(10)	–129 (12)	2033 (9)	6442 (8)
C(11)	–915 (14)	1573 (10)	6760 (9)
C(12)	1910 (12)	2045 (8)	4357 (9)
C(13)	2147 (14)	1554 (10)	3699 (9)
C(21)	9253 (37)	7500	898 (26)
C(22)	9145 (34)	7500	1523 (25)
Cl(1)	226 (11)	2500	1904 (8)
O(11)	1254 (22)	2500	1841 (14)
O(12)	–103 (19)	3034 (15)	1481 (12)
O(13)	234 (29)	2500	2544 (22)

Results and Discussion

Syntheses. In the solid state, bis(dimethylglyoximato)copper(II) is a binuclear centrosymmetric complex, $[Cu_2(dmgH)_4]$.[23] It dissolves in methanol in presence of an amine, viz. triethylamine, with the concomitant formation of a monomeric species, at least

---

(21) Sheldrick, G. M. SHELXTL PLUS program package 3. Universität Göttingen, 1988. Computations were carried out on a Microvax II Computer.

(22) *International Tables for X-ray Crystallography*; Kynoch: Birmingham, England, 1974; Vol. 4.

(23) Vaciago, A.; Zambonelli, L. *J. Chem. Soc. A* **1970**, 218.

Table III. Selected IR Spectral Data[a]

compound	ν/cm^{-1}	
$[Cu_2L_2Cu(dmg)_2](ClO_4)_2$ (**1**)	ν(CN)	1581 s (sh)
	ν(NO)	1216 s (sh)
$[Cu_2L_2Cu(dmg)_2Br](ClO_4)\cdot CH_3OH$ (**4**)	ν(CN)	1576 s (sh)
	ν(NO)	1216 s (sh)
$[Cu_2L_2Cu(dmg)_2Br]PF_6$	ν(CN)	1577 s (sh)
	ν(NO)	1211, 1097 s (sh)
	$\nu(PF_6)$	840 vs, 558 m (sh)
$[Cu_2L_2Ni(dmg)_2](ClO_4)_2\cdot 2H_2O$ (**2**)	ν(OH)	3505 m (br)
		1610 w (br)
	ν(CN)	1573 m (sh)
	ν(NO)	1228 s (sh)
$[Cu_2L_2Ni(dmg)_2]Br(PF_6)\cdot 2H_2O$ (**5**)	ν(OH)	3625 m (sh)
		3414 s (br)
		1610 w (br)
	ν(CN)	1564 s (sh)
	ν(NO)	1224 s (sh)
	$\nu(PF_6)$	845 vs, 558 s (sh)
$[Cu_2L_2Pd(dmg)_2](ClO_4)_2\cdot 2H_2O$ (**3**)	ν(OH)	3528 m (br)
	ν(CN)	1561 s (sh)
	ν(NO)	1235 s (sh)
$[Cu_2L'_2(OH_2)_2Cu(dmg)_2](ClO_4)_2$ (**6**)	ν(OH)	3441 m (br)
	ν(CN)	1579 s (sh)
	ν(NO)	1207 s (sh)
$[Cu_2L'_2(OH_2)_2Pd(dmg)_2](ClO_4)_2$ (**7**)	ν(OH)	3452 s (br)
		1634 m (br)
	ν(CN)	1567 s (sh)
	ν(NO)	1235 s (sh)

[a] Key: vs = very strong; s = strong; m = medium; w = weak; sh = sharp; br = broad.

Table IV. Electronic Spectral Data for Homo- and Heterotrinuclear Complexes in Acetonitrile at Ambient Temperature

complex	λ_{max}/nm (ϵ/M^{-1} cm^{-1})
$[Cu_2L_2Cu(dmg)_2](ClO_4)_2$ (**1**)	342 sh (~24 360), 433 sh (~6990), 467 sh (~6750), 565 (~1670)
$[Cu_2L_2Cu(dmg)_2Br]ClO_4\cdot CH_3OH$ (**4**)	341 sh (~11 885), 432 (~3115), 469 (~2952), 560 (~1920)
$[Cu_2L'_2(OH_2)_2Cu(dmg)_2](ClO_4)_2$ (**6**)	346 sh (~13 050), 418 sh (~4080), 471 sh (~3775), 543 sh (~2912)
$[Cu_2L_2Ni(dmg)_2](ClO_4)_2\cdot 2H_2O$ (**2**)	~362 sh (~6480), 424 sh (~2280), 469 sh (~1520), 560 sh (~550), 960 br (~35)
$[Cu_2L_2Ni(dmg)_2]Br(PF_6)\cdot 2H_2O$ (**5**)	~439 sh (~2340), ~480 sh (~1638), 601 sh (~445), 780 (91), 960 sh (~50)
$[Cu_2L_2Pd(dmg)_2](ClO_4)_2\cdot 2H_2O$ (**3**)	422 sh (~2850), 640 (216), 795 sh (~100), 1018 br (~56)
$[Cu_2L'_2(OH_2)_2Pd(dmg)_2](ClO_4)_2$ (**7**)	418 sh (~2650), 608 (281), 772 sh (~164)

in part, as is evidenced from the formation of the trinuclear copper(II) complexes. The function of added amine is to provide a basic medium needed for the deprotonation of the O···H···O groups present in the solid $Cu_2(dmgH)_4$ with both copper ions in square-pyramidal environments. The presumably square-planar dianionic $Cu(dmg)_2^{2-}$ produced in this way can now function as a bridging ligand for the coordinative unsaturated CuL^{2+} or CuL'^{2+} units. In the presence of perchlorate anions, dark-brown crystals of **1** and **6** are assembled in this manner in good yields (80%). The same type of reaction using copper bromide as a starting material affords complex **4** with all three copper ions in square-based pyramidal environments, a bromide ion being coordinated to the central copper atom.

The yields of the reactions using $Ni(dmg)_2^{2-}$ or $Pd(dmg)_2^{2-}$ anions as bridging ligands are lower (≈65%), since the deprotonation reaction in methanol does not proceed readily to the right-hand side of the

$$M(dmgH)_2 + 2Et_3N \rightleftarrows M(dmg)_2^{2-} + 2Et_3N^+H$$

equilibrium. Hence, an excess of triethylamine is used in the synthetic procedure for the heterotrinuclear complexes with Ni(II) or Pd(II) as the central atom to avoid the coprecipitation of the red $Ni(dmgH)_2$ or yellow-orange $Pd(dmgH)_2$ with the desired products.

Infrared Spectra. The presence or absence of certain bands in the generally complicated IR spectra have been utilized to establish the nature of the complexes. Relevant bands are listed in Table III. All of the perchlorate salts show strong bands near 1090–1100 (antisymmetric stretch) and sharp bands at 620–625 cm^{-1} (antisymmetric bend), indicative of uncoordinated perchlorate anions.

Since the spectra of all complexes **1**–**7** are quite similar, the discussion is confined to the most important vibrations of the 4000–400-cm^{-1} region in relation to the structure. The metal *vic*-dioximes, $Cu(dmgH)_2$, $Ni(dmgH)_2$, and $Pd(dmgH)_2$, have appreciable IR absorption in the region of 2300 cm^{-1} due to the OH stretching vibrations of the hydrogen-bonded OHO group.[24] These absorptions are missing in the spectra of the trinuclear complexes, indicating that the enolic hydrogen atoms are lost on chelation.

The medium strong bands at 1207–1235 cm^{-1} in the trinuclear complexes are assignable to the NO stretching vibration. $M(dmgH)_2$ [M = Cu(II), Ni(II), Pd(II)] complexes exhibit two bands of medium intensity at 1210–1255 and 1080–1102 cm^{-1} that are assignable to the NO stretch on the basis of the earlier reports.[24] The second NO IR absorption could not be observed in our trinuclear complexes because of the superposition with the bands originating from the perchlorate anions. However, for the hexafluorophosphate salt of the cation in complex **4**, the second NO stretch was identified unambiguously at 1097 cm^{-1}.

The ν(CN) vibration is assigned to the intense band in the wavenumber region 1561–1581 cm^{-1}; the band appears at 1561 cm^{-1} for the Cu_2Pd (**3**) complex and at 1581 cm^{-1} for the Cu_2Cu (**1**) complex. The ν(CN) vibration is situated at a significantly higher frequency than that for the corresponding bis(dimethylglyoximato)metal(II), where these vibrations are found at 1543 cm^{-1} for Cu(II) and 1546 cm^{-1} for Pd(II). This is in accord with the concept that on trinuclear complex formation the positively charged $(C_9H_{21}N_3)Cu^{2+}$ or $(C_6H_{16}N_2)Cu^{2+}$ unit stabilizes the negative charge on oxygen of the oximate[25] function and thus increases the double bond character of the CN bond, which is expressed as a rise in the frequency. Of all the complexes investigated, complex **3**, $Cu^{II}Pd^{II}Cu^{II}$, shows the lowest frequency for the ν(CN) vibration, denoting that, in the chelate ring of this complex, more electron delocalization has taken place. The frequency shift of the cyanide vibration from 1561 to 1581 cm^{-1} is also a demonstration of the M → N=C donor π-bond formation, and the strength of the π-bond is characterized in each system by the frequency of the ν(CN) vibration as well.

Electronic Spectra. The optical spectra for the trinuclear complexes have been measured in the range 300–1200 nm. The absorption maxima with the corresponding extinction coefficients in acetonitrile solutions are given in Table IV. The spectra of the homotrinuclear copper(II) complexes are dominated by charge-transfer transitions in the UV–vis regions.

Metal to ligand charge-transfer (MLCT) absorptions can occur in complexes where unsaturated ligands like dimethylglyoxime, which contain empty antibonding π-orbitals, are bonded to oxidizable metals. Judged on the basis of high extinction coefficients, the peaks and shoulders between 300 and 500 nm are ascribed to these charge-transfer transitions. The transitions are thought to be $d_{x^2-y^2}$–π_{oxime}* in character and occur at central Cu(II) centers of complexes **1**, **4**, and **6**. Similarly, for complexes **2**, **3**, **5**, and

---

[24] (a) Blinc, R.; Hadzi, D. *J. Chem. Soc. A* **1958**, 4536. (b) Burger, K.; Ruff, I.; Ruff, F. *J. Inorg. Nucl. Chem.* **1965**, *27*, 179. (c) Caton, J. E.; Banks, C. V. *Inorg. Chem.* **1967**, *6*, 1670.

[25] Chakrovorty, A. *Coord. Chem. Rev.* **1974**, *13*, 1.

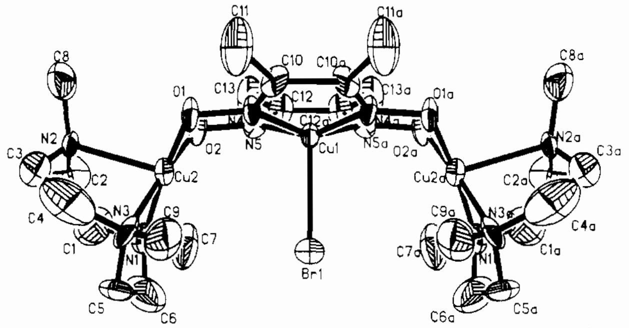

Figure 1. ORTEP drawing of the monocation $[L_2Cu_2(dmg)_2CuBr]^+$ (**4**).

7, the CT bands occurring at the central Ni(II) or Pd(II) center are assigned to $^1A_{1g}$–π_{oxime}* transitions.

A medium band or shoulder is found at 565 nm for **1**, at 560 nm for **4**, and at 543 nm for **6** on the low-energy side of the charge-transfer bands for the homotrinuclear copper complexes. This transition is thought to be of ligand field nature. The extinction coefficient of this shoulder is large, in spite of the Laporte g $\nleftrightarrow$ g selection rule, because of the extensive mixing of the metal d orbitals and the ligand orbitals and because of their proximity to other charge-transfer bands.

The broad band at ≈960 nm of complex **2** is also of ligand field origin, probably at the 6-fold coordinated Ni(II) center, which should ve viewed correctly as cis-planar with C_{2v} symmetry, with the fifth and sixth coordination positions being occupied by water molecules. More about the 6-fold coordination of the nickel(II) center in complexes **2** and **5** will be discussed with the magnetic susceptibility data (vide infra).

The peak at 780 nm of complex **5** needs special discussion. We think that this is a d–d band centered at the central six-coordinated Ni(II) ion (C_{2v}), the fifth and sixth position being occupied by a bromide and a water molecule. This assignment is based on the relative sharpness, the low extinction coefficient, and the position of the band in the electronic spectrum.

All other shoulders and peaks are definitely of spin-allowed d–d transitions in nature and strongly indicate the presence of five-coordinate copper(II) ions; this is in complete accord with our earlier observations[16a] of Cu(II) chemistry with this macrocyclic amine.

It has been shown by Hathaway[26] that it is possible to predict the stereochemistry of the local copper(II) environment in Cu(II) complexes of unknown crystal structure from the positions and intensities of d–d transitions of CuX_5 chromophores. In general trigonal bipyramidal complexes with $^2A'_1$ ground states exhibit a single, relatively intense band at (12 500 ± 1500) cm^{-1}; on the other hand, the electronic spectra of square-based pyramidal complexes consist of two clearly resolved bands covering the range (15 000 ± 2000) cm^{-1}. On the basis of the above arguments, a pseudo-square-pyramidal geometry is assigned to all terminal copper(II) centers in complexes listed in Table IV rather than a trigonal-bipyramidal geometry.

Molecular Structure of $[L_2Cu_2(dmg)_2CuBr]ClO_4 \cdot CH_3OH$ (4). The complex molecule consists of a monocationic trinuclear unit, a statistically disordered perchlorate anion, and a disordered methanol molecule. The cation together with the atomic labeling scheme used is shown in Figure 1. Selected bond lengths and angles are listed in Table V. Each copper ion is in a distorted square-pyramidal environment. The central copper ion Cu(1) is displaced by 0.4 Å from the mean basal plane of four nitrogen atoms of the dimethylglyoxime ligand toward the apical bromide ion. The Cu(1)–N(4) and Cu(1)–N(5) bond distances correspond to those of $Cu(dmgH)_2$.[23] The $[Cu(dmg)_2]^{2-}$ dianion bridges two terminal copper ions through its deprotonated oxime oxygen with a Cu(1)···Cu(2) separation of 3.381 (4) Å. The terminal copper ion, Cu(2), is coordinated to two nitrogen atoms, N(1) and N(3), of the cyclic amine, two oxygen atoms, O(1) and O(2) of the dmg^{2-} anion in the basal plane, and the third nitrogen atom, N(2), of the cyclic amine in the apical position. The Cu–N(av) and Cu–O(av) bond distances in the equatorial plane are 2.068 (17) and 1.909 (10) Å, respectively, and are considered as normal covalent bonds. The axial Cu(2)–N(2) bond is longer, 2.252 (13) Å, as is expected for square-pyramidal complexes of copper(II) and as has been observed earlier.[16] The terminal copper ions lie practically on the best basal plane comprising N(1)N(3)O(1)O(2) atoms and is displaced only 0.08 Å above the mentioned plane toward the apical nitrogen atom N(2) of the macrocyclic amine. The trinuclear skeleton is not coplanar, but is slightly butterfly shaped. The angle Cu(2)–Cu(1)–Cu(2a) is 152°, with a Cu(2)···Cu(2a) separation of 6.56 Å.

Table V. Selected Bond Distances (Å) and Angles (deg) for $[L_2Cu_2(dmg)_2CuBr]ClO_4 \cdot CH_3OH$ (**4**)

Cu(1)–Br(1)	2.571 (4)	Cu(2)–O(1)	1.907 (10)
Cu(1)–N(4)	1.966 (12)	Cu(2)–O(2)	1.911 (10)
Cu(1)–N(5)	1.958 (12)	Cu(2)–N(1)	2.054 (17)
Cu(1)–N(4A)	1.966 (12)	Cu(2)–N(2)	2.252 (13)
Cu(1)–N(5A)	1.958 (12)	Cu(2)–N(3)	2.082 (18)
Br(1)–Cu(1)–N(4)	100.2 (4)	O(1)–Cu(2)–O(2)	93.8 (4)
Br(1)–Cu(1)–N(5)	103.6 (4)	O(1)–Cu(2)–N(1)	171.6 (6)
N(4)–Cu(1)–N(5)	94.5 (5)	O(2)–Cu(2)–N(1)	91.4 (6)
Br(1)–Cu(1)–N(4A)	100.2 (4)	O(1)–Cu(2)–N(2)	103.9 (5)
N(4)–Cu(1)–N(4A)	80.1 (7)	O(2)–Cu(2)–N(2)	95.8 (5)
N(5)–Cu(1)–N(4A)	156.2 (5)	N(1)–Cu(2)–N(2)	82.1 (6)
Br(1)–Cu(1)–N(5A)	103.6 (4)	O(1)–Cu(2)–N(3)	91.0 (6)
N(4)–Cu(1)–N(5A)	156.2 (5)	O(2)–Cu(2)–N(3)	174.1 (6)
N(5)–Cu(1)–N(5A)	81.0 (7)	N(1)–Cu(2)–N(3)	83.4 (8)
N(4A)–Cu(1)–N(5A)	94.5 (5)	N(2)–Cu(2)–N(3)	86.5 (6)

Table VI. EPR Data for Trinuclear Complexes

complex	T/K	$g_\parallel$	$g_\perp$	$\langle g \rangle$
1	10.1	2.217	2.100	2.139
4	10.1	2.247	2.068	2.127
6	10.1	2.248	2.050	2.116
2	10.9	quasi-isotropic		2.137
3	77.0	quasi-isotropic		2.075
5	8.9	quasi-isotropic		2.146
	10.1	quasi-isotropic		2.146
	77.0	quasi-isotropic		2.146
7	13.5	quasi-isotropic		2.140
	77.0	quasi-isotropic		2.140

Results from Simulation

1: $g = 2.230, 2.100, 2.090$; LW = 80, 65, 30 G

4: $g = 2.260, 2.070, 2.070$; LW = 50, 30, 25 G

6: $g = 2.250, 2.040, 2.050$; LW = 50, 15, 10 G

EPR Spectra. The X-band EPR spectra of complexes **1**–**7** were recorded on powder samples at various temperatures. In order to avoid texture effects due to orientation of crystallites in the magnetic field, the powder sample was suspended in the nonsolving liquid hexane, which formed a rigid matrix on cooling. The spectra are typical for $S = {}^1/_2$ spin systems; the g values obtained are summarized in Table VI. Spectra for **1**, **4**, and **6** at 10.1 K together with the simulated spectra are shown in Figure 2. Reasonable results from the simulation could be obtained by considering only three separated g values. The computer program[33] calculates the absorption pattern of spin packets for given directions of the magnetic field with respect to the molecular axes, using microwave frequency, effective g values and line widths as parameters. The line shapes of spin packets chosen were Lorentzian. The g values of the simulated spectra are in accord with the g values listed in Table VI. Complexes **1**, **4**, and **6** exhibit a ground state of total spin $S = {}^1/_2$. Temperature-dependent measurements up to 100 K show that the ground state is energetically well-separated from excited doublet and quartet states. Magnetic susceptibility measurements, given in the following section, support the coupling scheme of Figure 4, which visualizes the contribution of the three individual spins S_i, (i = 1, 2, 3) to the ground doublet $|S = {}^1/_2, S^* = 1\rangle$, with $S^* = S_1 + S_3$ and

---

(26) (a) Hathway, B. J.; Tomlinson, A. A. G. *Coord. Chem. Rev.* **1970**, *5*, 1. (b) Hathway, B. J.; Billing, D. E. *Coord. Chem. Rev.* **1970**, *5*, 143. (c) Hathway, B. J. *Struct. Bonding (Berlin)* **1984**, *57*, 55.

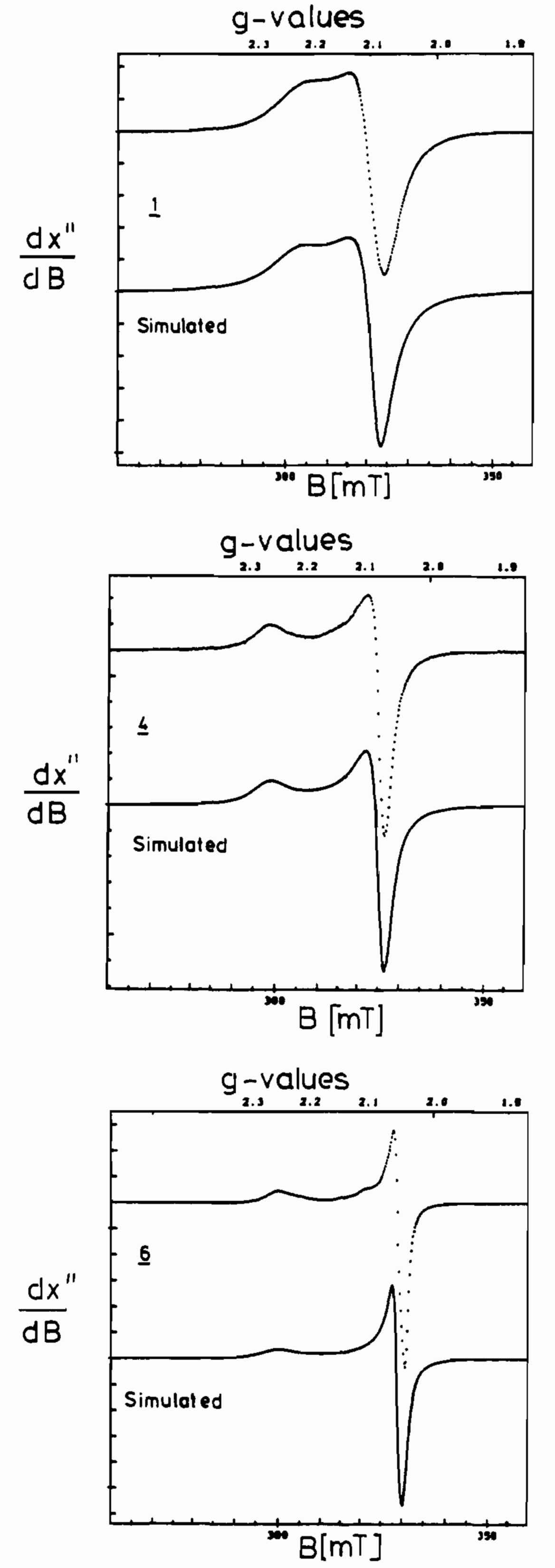

Figure 2. X-Band EPR spectra of **1**, **4**, and **6** at 10.1 K.

$S = S^* + S_2$. From the usual spin-projection techniques[27] one derives the **g** tensor for the ground state

$$\mathbf{g} = \tfrac{2}{3}g_1 - \tfrac{1}{3}g_2 + \tfrac{2}{3}g_3$$

in the terms of the local **g** tensors. The coefficients ${}^2/_3$ and $-{}^1/_3$ show that the local values g_1 and g_3 of the terminal Cu ions dominate the values of g of the trinuclear complex. If we assume that the g components of the individual sites do not differ too much, at least the numerical order of the components $g_\parallel$ and $g_\perp$, measured by EPR, is determined by the terminal copper ions. This allows us to draw some conclusions about the highest occupied 3d orbitals of Cu(II) ions in the trimer. The EPR spectra of mononuclear copper(II) complexes exhibiting two types of g values, $g_\parallel \neq g_\perp$, have been used[26] to distinguish unambiguously between $(d_{x^2-y^2})^1$ and $(d_{z^2})^1$ ground states; the $d_{x^2-y^2}$ orbital yields $g_\parallel > g_\perp$, while d_{z^2} yields $g_\perp > g\|$. The homotrinuclear copper(II) complexes studied here show a pronounced peak ($g \approx 2.10$) and a broad peak ($g \approx 2.20$), typical of a d^9 complex possessing axial symmetry with the unpaired electron present in a $d_{x^2-y^2}$ orbital. The spectra of **1**, **4**, and **6** do not show any half-field ($\Delta M_s = 2$) transition or fine structure and look like a spectrum associated with isolated $S = {}^1/_2$ states.

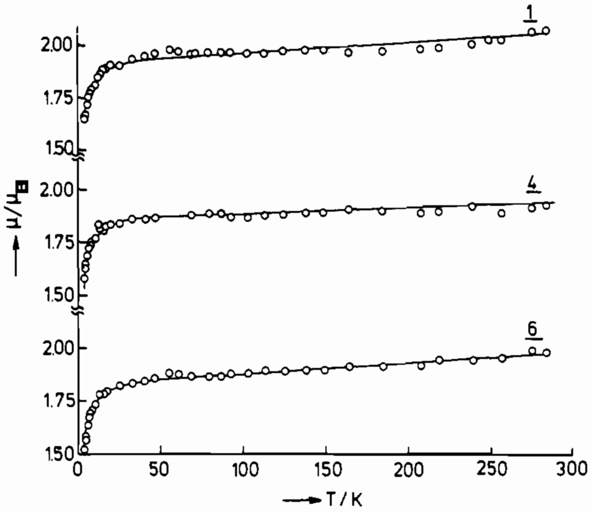

Figure 3. Plots of magnetic moment vs. temperature for solid **1**, **4**, and **6**. The solid lines represent the best least-squares fits of the experimental data to the theoretical equation.

Energy	Spin (S,S*)
$-J - 1/2\,J_{13}$	(3/2,1)
$3/2\,J_{13}$	(1/2,0)
$2J - 1/2\,J_{13}$	(1/2 ,1)

Figure 4. Energy levels of a spin coupled linear homotrinuclear complex, $\{S_i = {}^1/_2\}$, i = 1, 2, 3. S is the total spin and $S^* = S_1 + S_3$.

For complexes **2**, **3**, **5**, and **7**, spectra with quasi-isotropic g values are obtained. They also do not show any half-field signal or fine structure. The averaged $\langle g \rangle$ values measured by EPR are in fair agreement with the values obtained by the fitting procedure of the magnetic susceptibility data (vide infra).

Magnetic Susceptibility. Magnetic susceptibility data for solid samples of **1**, **4**, and **6** were collected in the temperature range 4.2–284 K, and the data are displayed in Figure 3 as μ_{eff} vs. temperature. The μ_{eff}/trinuclear complex values vary only slightly over the temperature range from 1.72 μ_B at 6.2 K to 2.07 μ_B at 284 K for **1**, from 1.73 μ_B at 7.1 K to 1.93 μ_B at 284 K for **4**, and 1.74 μ_B at 11.2 K to 1.99 μ_B at 284 K for **6**.

Three copper atoms in **4** are arranged at the corners of an isosceles triangle (see the X-ray structure), each assumed to be in a $^2B_1$ ground state with no contribution from orbital angular momentum. The structures of **1** and **6** are presumed to be very similar to that of **4**. Accordingly, the susceptibility data were fitted by means of least-squares methods to the theoretical expression[7] for χ_M for a linear or a bent trinuclear complex with $J_{12} = J_{23} = J$ and J_{13}, which results from the spin Hamiltonian

$$\hat{H} = -2J[\hat{S}_1\cdot\hat{S}_2 + \hat{S}_2\cdot\hat{S}_3] - 2J_{13}(\hat{S}_3\cdot\hat{S}_1)$$

for an isotropic magnetic exchange from $S_1 = S_2 = S_3 = {}^1/_2$. Thus

---

[27] Banci, L.; Bencini, A.; Gatteschi, D. *Inorg. Chem.* **1983**, *22*, 2681.

Table VII. Magnetic Parameters for Homo- and Heterotrinuclear Copper(II) Complexes

compound	J/cm^{-1}	g_{mag}	Θ/K	P
$[Cu_2L_2Cu(dmg)_2](ClO_4)_2$ (**1**)	−376	2.20	−1.1	0.014
$[Cu_2L_2Ni(dmg)_2(OH_2)_2](ClO_4)_2$ (**2**)	−2.6	2.02	0	0
$[Cu_2L_2Pd(dmg)_2](ClO_4)_2\cdot 2H_2O$ (**3**)	−36	2.06	0	0.01
$[Cu_2L_2Cu(dmg)_2Br](ClO_4)\cdot CH_3OH$ (**4**)	−448	2.10	−0.2	0.01
$[Cu_2L_2Ni(dmg)_2(OH_2)_2]Br(PF_6)$ (**5**)	−1.3	2.18	−0.9	0.014
$[Cu_2L'_2(OH_2)_2Cu(dmg)_2](ClO_4)_2$ (**6**)	−345	2.12	−1.4	0.01
$[Cu_2L'_2(OH_2)_2Pd(dmg)_2](ClO_4)_2$ (**7**)	−0.8	2.16	0	0

J represents the exchange between adjacent copper atoms and J_{13} describes the interaction between the terminal copper nuclei (1 and 3) within the trinuclear complex, as shown pictorially below:

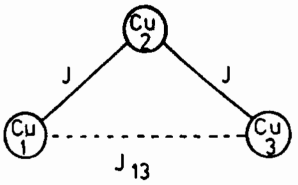

A correction for a small amount of paramagnetic impurity ($S = {}^1/_2$) was also taken into account by adding a Curie law expression to the formula

$$\chi_{\text{calcd}}^{\text{Cu}_3\,\text{cluster}} = (1 - P)\left[\frac{C}{T - \Theta} f(J, J_{13}, T)\right] + P\frac{C}{T} + \text{TIP}$$

where P is the amount of the paramagnetic impurity, $C = Ng^2\mu_B{}^2/k$, $f(J,J_{13},T)$ is as given in the literature,[7] and TIP = 60×10^{-6} cm^{-3} mol^{-1} for each copper atom. The experimental values of χ have been fitted to this equation by treating g, J, J_{13}, and Θ as adjustable parameters and also by holding $J_{13} = 0$ and allowing g, J, and Θ to vary. The resulting best fits are shown as the solid lines in Figure 3. The quality of the fit does not depend on J_{13}, and hence the fits with $J_{13} = 0$ have been accepted to be more plausible. That J_{13} cannot be determined from the susceptibility data but that J can be obtained with a reasonable accuracy has also been pointed out earlier.[27] The exchange coupling constants together with the other parameters resulting from the fits of the magnetic data are listed in Table VII. At temperatures below ≈10 K, the experimental magnetic moments for compounds **1**, **4**, and **6** fall below the expected theoretical value of 1.73 μ_B, obvious in Figure 3. This deviation may be the result of weak antiferromagnetic interactions between neighboring trinuclear complexes.

The magnitudes of the exchange integrals J between neighboring cupric ions are very large to be deduced very accurately, since the susceptibility at temperatures much lower than $|J|$ is independent of J. The proper conclusion here is that **1**, **4**, and **6** exhibit strong antiferromagnetic coupling with doublet ground states and can be arranged on the basis of their spin coupling in the following way: **4** > **1** ≈ **6**.

The environment around terminal copper(II) ions is square pyramidal with $(d_{x^2-y^2})^1$ ground states. The strong antiferromagnetic interaction in **4** can be interpreted by considering that magnetic orbitals of Cu(II) ions, $d_{x^2-y^2}$, point from the metal toward the four nearest neighbors and overlap on either side of the bridging glyoximato ligand, which favors a strong antiferromagnetic interaction. Weaker interactions in **1** and **6** can be rationalized by envisaging that the geometry around terminal copper(II) ions has deviated from a square pyramid toward a trigonal bipyramid, but is still far from a purely trigonal-bipyramidal chromphore as evidenced by EPR spectra. With increasing trigonal character of the CuN_2O_3 chromophore in **6** and of the CuN_2O_2 in chromophore in **1**, the d_{z^2} character of the magnetic orbital increases and hence a reduction in the magnetic exchange interaction is observed.

The Cu–Cu separation of 3.379 Å in **4** is so large that the exchange integral cannot originate from direct Cu–Cu interaction. Thus, the observed spin coupling is likely to arise through a superexchange mechanism operating via the Cu–O–N–Cu–N–O–Cu linkages. A similar argument should also account for the magnetic exchange pathways in the case of **1** and **6**, tricopper(II) complexes.

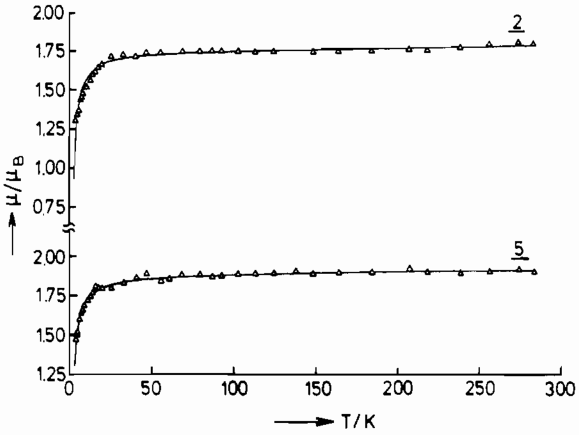

Figure 5. Plots of μ_{eff}/Cu vs T for solid **2** and **5**. The solid lines represent the best least-squares fits of the experimental data to the theoretical equation.

A similar trinuclear copper(II) complex containing bipyridyl as the capping ligands, $[(bpy)_2(CH_3OH)_2Cu_2Cu(dmg)_2](NO_3)_2$, with the terminal copper ions in distorted square-pyramidal environments has recently been described.[19] The basal planes of the Cu(II) ions in the reported compound are nearly coplanar, and "the $-J$ value larger than 300 cm^{-1}" has been found.[19] Interestingly, in our compound **4**, the $Cu(1)N_2O_2Cu(2)$ bridging networks are not planar and also the three basal planes containing the copper(II) ions are not coplanar (Figure 1), which should diminish the overlap between the magnetic orbitals. But the spin exchange interactions in **1**, **4**, and **6** are at least very similar, if not stronger (Table VII), than those for the bipyridyl compound of Okawa et al.[19] These observations might suggest that the unusually large spin exchange interaction in these trinuclear Cu(II) complexes is not the result of any special geometrical features but is related to the electronic structure of the bridging dimethylglyoximato ions.

The following drawing shows the orientation of the relevant orbitals for the mechanism of interaction.

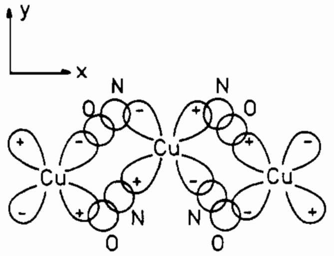

Of the two possible orbital exchange pathways, σ- and π-exchanges, the σ-pathway is considered to provide the dominant antiferromagnetic interaction. Because of the symmetry properties of the σ-interaction, $d_{x^2-y^2}$ orbitals on the Cu(II) ions and σ orbitals on the bridging oxygen and nitrogen atoms are involved in the exchange pathway for unpaired spin density. That the rational description of the antiferromagnetic exchange mechanism in ours and Okawa and co-workers'[19] trinuclear copper(II) complexes is σ-exchange is evident from the nondependence of the angles between the basal planes of copper(II) ions on effective orbital overlap, i.e. the magnitude of the exchange interaction. The π-pathway is expected to lead to exchange interactions whose magnitudes should be dependent on the angles between the copper basal planes in which the unpaired spins are located.

For three interacting centers with $S_i = {}^1/_2$, i = 1, 2, 3, the resulting spin multiplets $|S, S^*\rangle$ are two doublets ($|{}^1/_2, 1\rangle$, $|{}^1/_2, 0\rangle$) and one quartet ($|{}^3/_2, 1\rangle$), where S^* is defined through the relation $S^* = S_1 + S_3$ and S is the total spin. In complexes **1**,

4, and **6**, there are two equivalent copper ions, Cu(1) and Cu(3), and hence the two spin doublets are not mixed. The energies of the three spin states are shown schematically in Figure 4. From the magnetic susceptibility data for **4**, it can be derived that the first excited spin doublet state is positioned at about 900 cm^{-1} above the doublet ground state.

Magnetic Propeties of 2 and 5. A complete X-ray structure determination of **2**, $[L_2Cu_2(dmg)_2Ni](ClO_4)_2\cdot 2H_2O$, was not possible because of crystal disorder, but a qualitative investigation showed that two water molecules are directly attached to the nickel center in a cis-planar fashion (local symmetry at Ni center is C_{2v}), yielding a six coordinate Ni compound that should be formulated as $[LCu(\mu\text{-}\{(dmg)_2Ni(cis\text{-}OH_2)_2\})CuL](ClO_4)_2$. It has also been observed from the qualitative X-ray structure determination that the three metal centers do not lie in a plane, but a bent structure is attained as schematized below:

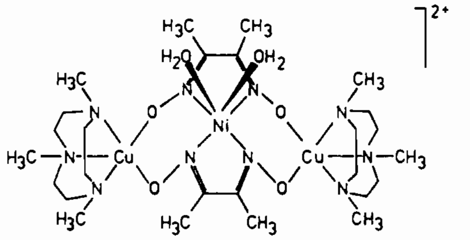

The magnetic susceptibility data for **2** and **5** are shown in Figure 5 as the effective magnetic moment (μ_{eff}/Cu) plotted as a function of temperature. The μ_{eff}/Cu values over the temperature range vary from 1.80 μ_B at 284 K to 1.31 μ_B at 4.2 K for **2** and from 1.91 μ_B at 284 K to 1.47 μ_B at 4.2 K for **5**. The data were fitted by means of least-squares methods to the formula (using a Weiss constant Θ) for the paramagnetic susceptibility[28] that results from the spin Hamiltonian ($\hat{H} = -2J\hat{S}_1\hat{S}_3$) for an isotropic magnetic exchange with $S_1 = S_3 = {}^1/_2$. The least-squares fits are also shown in Figure 5. Attempts to fit the magnetic data for **2** and **5** with spin systems $S_1 = S_3 = {}^1/_2$ and $S_2 = 1$ were unsuccessful, but a very good quality fitting is obtained by considering $S_1 = S_3 = {}^1/_2$ and $S_2 = 0$. The results are summarized in Table VII. Diagmagnetism of $[Ni(dmg)_2(OH_2)_2]^{2-}$ ion (C_{2v} or cis-planar) means that the in-plane field of the nitrogen atoms is much stronger than the cis-axial perturbations from oxygen atoms of water ligands to produce a singlet ground state for Ni(II). In D_{2h} symmetry (trans-planar), a larger in-plane field is necessary to produce a singlet ground state than that in the D_{4h} (square-planar) or C_{2v} (cis-planar) case. The systems with D_{2h} symmetry are more susceptible to *z*-axial perturbations than the D_{4h} or C_{2v} cases; i.e., a triplet ground state is more readily obtained with D_{2h} symmetry. These facts have been known for Ni(II) chemistry for many years.[29] Thus a good quality fitting of magnetic data for **2** and **5** with diamagnetic six-coordinate Ni(II) is not surprising.

The shape of the susceptibility plot (Figure 6) for **3** and **7** reveals a behavior typical of an antiferromagnetically coupled binuclear compound with the maxima at ≈56 K for **3**. No maxima is observed in the susceptibility vs temperature plot for **7**, indicating diminished exchange interactions relative to those in complex **3**. The μ_{eff}/Cu values over the temperature range vary from 0.18 μ_B at 4.2 K to 1.75 μ_B at 284 K for **3** and from 1.71 μ_B at 4.2 K to 1.93 μ_B at 284 K for **7**. The magnetic parameters (Table VII) are estimated as *g* and *J* from a least-squares fitting of the susceptibility data by the Bleaney–Bowers equation[28] for simple copper(II) dimers, where 2*J* is the energy difference between the singlet and triplet states. The solid lines in Figure 6 represent these fits. The Cu···Cu distance in **3** is estimated to be ≈7.6 Å, based on the Cu···Cu separation of a similar complex for which structural data are available.[19] In full accord with expectation,[16f] medium–strong antiferromagnetic interaction is observed for **3** with $2J = -72$ cm^{-1}. Thus the following structure is envisaged for **3**. Each copper ion is located in distorted square-pyramidal surroundings with two nitrogen atoms of the cyclic amine and two oxygen atoms of the dimethylglyoximato dianion in the basal plane and the third nitrogen atom of the 1,4,7-trimethyl-1,4,7-triazacyclononane in the apical position. The square-planar $[Pd(dmg)_2]^{2-}$ ion (hence $S_{Pd} = 0$) bridges two copper ions through its deprotonated oxime oxygens, and the trinuclear skeleton is nearly coplanar.

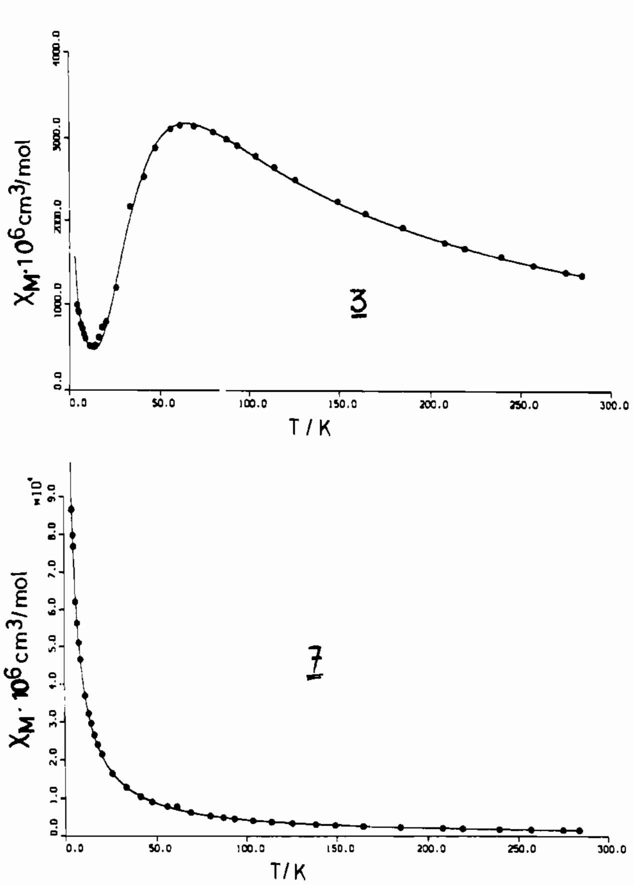

Figure 6. Plots of magnetic susceptibility vs temperature for solid **3** and **7**. The solid lines represent the best least-squares fits of the experimental data to the theoretical equation.

It is already known that the bonding of further ligands by a square-planar complex is much weaker with palladium than with nickel. Thus we conclude that the water molecules in **3** are not coordinated to the central Pd ion, resulting in a square-planar diamagnetic palladium(II) center (cf. complex **2**).

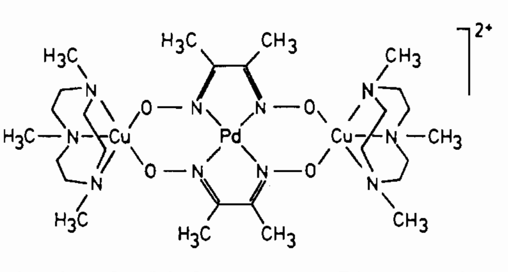

The trinuclear Cu–Pd–Cu skeleton in **7** is expected to be less coplanar than that in **3**, and the resulting poor effective overlap between the magnetic orbitals results in practically no coupling ($J = -0.8$ cm^{-1}) between spins of two copper centers through the multiple atom bridging ligands. That |*J*| values decrease significantly when the terminal ligands are changed from 1,4,7-trimethyl-1,4,7-triazacyclononane to *N,N,N′,N′*-tetramethylethylenediamine has also been observed earlier by us.[16a] It is particularly unfortunate that we have not yet been able to grow single crystals of **3** and **7** suitable for an X-ray investigation in order to confirm the rationalization of the magnetic properties of **3** and **7**.

---

(28) O'Connor, C. J. *Prog. Inorg. Chem.* **1982**, *29*, 203.

(29) Miller, J. R. In *Advances in Inorganic Chemistry and Radiochemistry*; Emeleus, H. J., Sharpe, A. G., Eds.; Academic Press: New York, 1962; Vol 4, p 133.

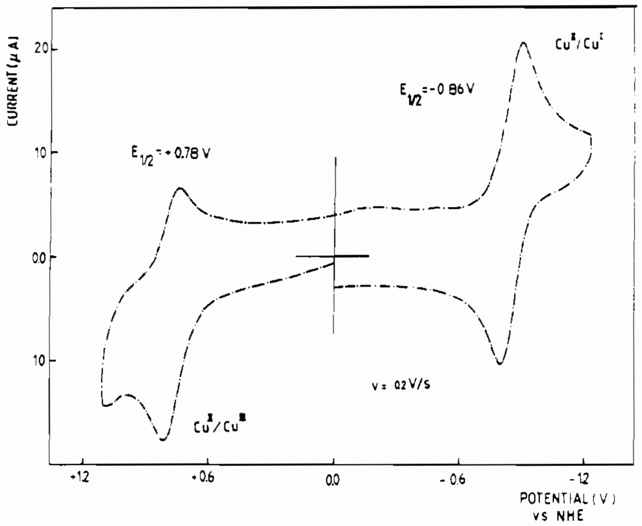

Figure 7. CV of $Cu(dmgH)_2$ in CH_2Cl_2 at a scan rate of 0.2 V s^{-1}.

Electrochemistry. The cyclic voltammogram of $Cu(dmgH)_2$ in CH_2Cl_2 (containing 0.1 M tetra-*n*-butylammonium hexafluorophosphate as supporting electrolyte at a glassy-carbon working electrode at $r = 0.2$ V/s is shown in Figure 7. Two quasi-reversible one-electron-transfer waves are detected in the potential range +1.16 to −1.24 V at $E_{1/2}^{ox} = +0.78$ V and $E_{1/2}^{red} = -0.86$ V vs NHE. The first process ($E_{1/2}^{ox}$) corresponds to the Cu(II)/Cu(III) couple. At slower scan rates (≤100 mV s^{-1}) a loss of cathodic current is observed, probably due to the slow decomposition of the oxidized Cu(III) form. The second ($E_{1/2}^{red}$) process has been assigned to the Cu(II)/Cu(I) couple. Similar redox chemistry has been reported for $Cu(dmgH)_2$ in aqueous solution.[30]

The cyclic voltammogram of **4** is shown in Figure 8. In the potential range +1.04 to −1.66 V vs. NHE, **4** shows one quasi-reversible one-electron-transfer wave at +0.60 V and an irreversible two-electron reduction at −1.32 V vs. NHE. An irreversible small oxidation wave is also observed at −0.86 V. On the second scan, another small oxidation peak at +0.1 V is observed. The products of this oxidative degradation have not been characterized to date. At all scan rates investigated (0.02–20 V s^{-1}), no evidence for ECE mechanism[31] is observed. The following redox scheme, containing the reversible formation of a mixed-valent $Cu^{II}Cu^{III}Cu^{II}$ species, has been established for the electrochemical behavior of complex **4**.

$$Cu^{II}Cu^{III}Cu^{II} \underset{-e^-}{\overset{+e^-}{\rightleftharpoons}} \underset{\mathbf{4}}{Cu^{II}Cu^{II}Cu^{II}} \xrightarrow{+2e^-}$$

$$Cu^{I}Cu^{I}Cu^{II} \rightarrow \text{products}$$

The cyclic voltammetric behavior of complex **1** at $r = 0.2$ V s^{-1} in the potential range +1.14 to −1.97 V vs NHE is also shown in Figure 8. The compound undergoes one quasi-reversible one-electron oxidation at $E_{1/2} = +0.73$ V and two reduction processes with an $E_rC_iE_i$-type mechanism (i.e. a single chemical reaction coupled with two electron-transfer steps). When this complex is cathodically scanned (0.0 to −1.95 V), the reduction peak at E^1_{pc} = =0.92 V and then the peak at $E^2_{pc} = -1.34$ V are observed. When the sweep is reversed at −1.95 V toward the anodic direction, a small oxidation wave is observed at $r \geq 0.05$ V s^{-1}; at $r < 0.05$ V s^{-1}, the irreversibility of the second reaction becomes dominant and no oxidation peak is observed. When the voltage scan is reversed before the second reduction peak (E^2_{pc}) starts to grow, the first reduction peak (E^1_{pc}) becomes a quasi-reversible one-electron process at $r \geq 1$ V s^{-1} with $E_{1/2} = -0.88$ V vs NHE. Furthermore, the $i_p/r^{1/2}$ values measured at $r \geq 1$ V s^{-1} for each peak are identical, indicating that the same number of electrons are transferred in each process. The $E_{qr}C_i$ mechanism[31] has been assigned to the process on the basis of the following trends: (a) i_{pc}/i_{pa} is less than one, but approaches a value of unity at the higher scan rates ($r \geq 1$ V s^{-1}); (b) E_{pc} only shifts slightly to more negative potentials on increasing r; (c) $i_{pc}/r^{1/2}$ values decrease slowly with increasing r.

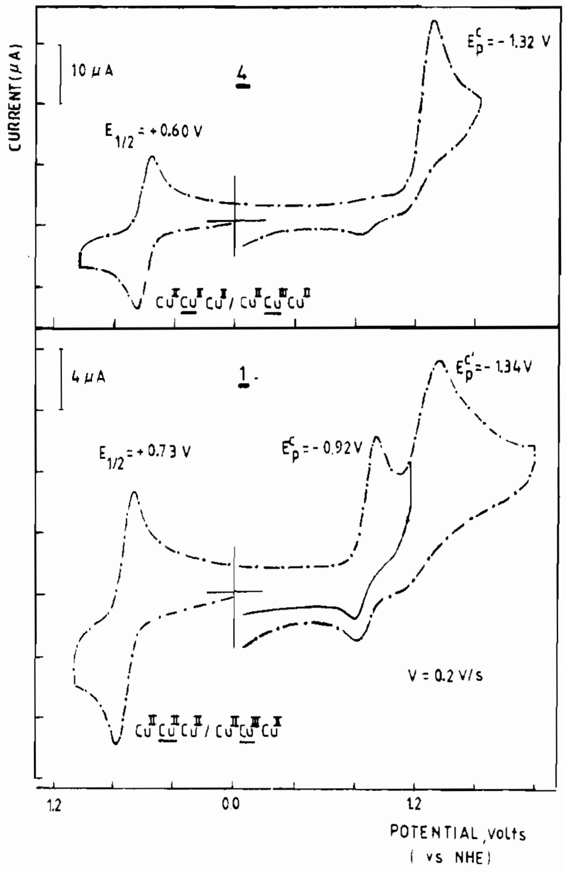

Figure 8. CV of **1** and **4** in CH_2Cl_2 at a scan rate of 0.2 V s^{-1}.

Thus, the above electrochemical behavior leads to the following reaction scheme:

positive potential

$$Cu^{II}Cu^{II}Cu^{II} \underset{+e^-}{\overset{-e^-}{\rightleftharpoons}} Cu^{II}Cu^{III}Cu^{II} \quad E_{1/2} = +0.73 \text{ V vs NHE}$$

negative potential

$$Cu^{II}Cu^{II}Cu^{II} \underset{-e^-}{\overset{+e^-}{\rightleftharpoons}} Cu^{II}Cu^{I}Cu^{II} \quad E_{1/2} = -0.88 \text{ V vs NHE}$$

$$Cu^{II}Cu^{I}Cu^{II} \rightarrow Z$$

$$Z + e^- \rightarrow \text{product} \quad E_{pc} = -1.34 \text{ V}$$

Compound **6** undergoes one quasi-reversible one-electron oxidation at $E_{1/2} = +0.95$ V vs NHE and a one-electron irreversible reduction at $E_p \approx -0.63$ V.

Concluding Remarks. The results described in the present paper show that bis(dimethylglyoxymato)metalate(II) dianions are capable of coordinating as a bridging ligand to give rise to various kinds of trinuclear complexes and can mediate a varying range of exchange, very weak to very strong antiferromagnetic, interactions. These materials are ideally suited for the study of intramolecular magnetic-exchange interactions. Recently another series of glyoximate-bridged heterotrinuclear complexes of general formula $[L_2Fe_2^{III}M^{II}(dmg)_3]^{2+}$ (M = Zn, Cu, Ni, Co, Fe, Mn) was obtained.[32]

---

(30) Sulfab, Y. *Polyhedron* **1989**, *8*, 2409.

(31) (a) Nicholson, R. S.; Shain, I. *Anal. Chem.* **1964**, *36*, 706. (b) Bard, A. J.; Faulkner, L. R. *Electrochemical Methods: Fundamentals and Applications*; John Wiley & Sons: New York, 1980.

(32) Chaudhuri, P.; Winter, M.; Fleischhauer, P.; Haase, W.; Flörke, U.; Haupt, H.-J. *J. Chem. Soc., Chem. Commun.* **1990**, 1728.

A moderately strong antiferromagnetic interaction ($2J = -72$ cm^{-1}) has been found for a compound (**3**) with an estimated Cu···Cu separation of ≈7.6 Å, and definitely, this is not the limit for the intramolecular magnetic interaction between two Cu(II) ions, provided the Cu(II) ions and the bridging ligand have the proper geometry.[16f] The mixed-valence species $Cu^{II}Cu^{III}Cu^{II}$ obtained by electrochemical oxidation seems to be stable on the voltammetric time scale, and hence, the chemical preparation of the oxidation products should be feasible.

Acknowledgment. Our sincere thanks are due to Prof. W. Haase (TH Darmstadt) for allowing us to use his Faraday balance. P.C. is grateful to Prof. K. Wieghardt for his generous help and interest.

Supplementary Material Available: Listings of intraligand bond distances and angles (Tables SI and SII), hydrogen atom coordinates (Table SIII), anisotropic thermal parameters (Table SIV), and crystal data (7 pages); a listing of observed and calculated structure factors (9 pages). Ordering information is given on any current masthead page.

---

(33) Twilfer, H.; Gersonde, K.; Christahl, M. *J. Magn. Reson.* **1981**, *44*, 470.

Contribution from the Fachbereich Chemie, Universität Dortmund, D-4600 Dortmund 50, Germany,
and Fachbereich Chemie, Universität-GH-Duisburg, D-4100 Duisburg, Germany

Preparation of the Nitryl Salts $ON(Cl)F^+AsF_6^-$, $ON(CF_3)F^+AsF_6^-$, and $HON(CH_2)CF_3^+SbF_6^-$ and Crystal Structure of $HON(CH_2)CF_3^+AsF_6^-$

Rolf Minkwitz,*[,†] Dirk Bernstein,[†] Hans Preut,[†] and Peter Sartori[‡]

Received June 19, 1990

The $ON(Cl)F^+AsF_6^-$ and $ON(CF_3)F^+AsF_6^-$ salts are prepared by oxidative fluorination of ONCl and $ONCF_3$ with $N_2F^+AsF_6^-$. Methylation of $ONCF_3$ with CH_3F and AsF_5 gives $ON(CH_3)CF_3^+AsF_6^-$, which in the solid state exists as the enol tautomer hydroxylimmonium salt $HON(CH_2)CF_3^+AsF_6^-$, triclinic, of space group $P\bar{1}$ with $a = 5.063$ (1) Å, $b = 7.757$ (3) Å, $c = 10.429$ (2) Å, $\alpha = 86.75$ (2)°, $\beta = 89.34$ (2)°, and $\gamma = 74.12$ (2)°. The framework of the cation is planar, with C–N bond lengths of 147.7 (5) and 127.3 (5) pm and an N–O distance of 137.2 (4) pm. The cation and anion have a short H···F contact of 166 (6) pm. An alternative method for the preparation of $ONF_2^+MF_6^-$ (M = As, Sb) was found involving the oxidative fluorination of ONF with $XeF^+MF_6^-$.

Introduction

Presently, only two nitryl cations exist: $ONCl_2^+$ and ONF_2^+. Their synthesis is specifically linked to the desired cation. The latter, ONF_2^+, is obtained from trifluoroamine oxide, ONF_3, and strong Lewis acids such as AsF_5 or SbF_5.[1,2] $ONCl_2^+$, which is isoelectronic with phosgene, $OCCl_2$, is formed in very poor yields as a $SbCl_6^-$ salt according to eq 1.[3] The salt is thermally stable up to 145 °C.[3]

$$NCl_3 + OSCl_2 + SbCl_5 \rightarrow ONCl_2^+SbCl_6^- + SCl_2 \quad (1)$$

In contrast, oxidative chlorination of ONCl by Cl_2/AsF_5 mixtures at −76 °C (eq 2) gives high yields of $ONCl_2^+AsF_6^-$, but

$$2ONCl + Cl_2 + 3AsF_5 \rightarrow 2ONCl_2^+AsF_6^- + AsF_3 \quad (2)$$

this compound is stable only below −78 °C. $ONCl_2^+SbF_6^-$, prepared in a similar manner, is also unstable.[4]

Attempts to prepare $ON(CF_3)_2^+SbF_6^-$ are reported in the literature.[5] One-electron transfer with $O_2^+SbF_6^-$ and PtF_6 should create the salt from the $ON(CF_3)_2$ radical. The high oxidation potentials of these systems, however, cause fission of the N–C bond, giving $NO^+SbF_6^-$ and byproducts.[5]

Although ab initio calculations show potential minima for NF_5 and even NF_6^-, assuming unusually long N–F bond distances,[6] neither thermolysis of $NF_4^+HF_2^-$ nor reaction of NF_4^+ salts with alkali-metal fluoride gives pentafluoroazoran. The reactions proceeded according to eqs 3 and 4.[7]

$$NF_4^+HF_2^- \rightarrow NF_3 + F_2 + HF \quad (3)$$

$$NF_4^+PF_6^- + CsHF_2 \rightarrow NF_4^+HF_2^- + CsPF_6 \quad (4)$$

$NCl_4^+AsF_6^-$, which has been synthesized by us recently,[8] decomposes similarly:

$$NCl_4^+AsF_6^- \xrightarrow[\text{IR matrix}]{\Delta} NCl_3 + AsF_5 + ClF \quad (5)$$

The thermal decomposition reaction of $ONF_2^+MF_6^-$ (M = As, Sb) proceeds differently. On heating, trifluoroamine oxide is formed, which attracts high interest with respect to bond theories.[6,9,10]

$$ONF_2^+MF_6^- \rightarrow ONF_3 + MF_5 \qquad M = As, Sb \quad (6)$$

Since to date neither mixed haloamine oxides nor their cations are known, we became interested in their syntheses.

Experimental Section

Materials and Apparatus. Volatile substances were handled in a high-vacuum line with greaseless stopcocks (Young). Solids were manipulated by Schlenk techniques. Experiments in anhydrous HF were conducted in KEL-F reactors with stainless steel valves (Hoke). Solvents SO_2 and CCl_3F were stored over CaH_2. AsF_5 and SbF_5 (Merck) were distilled repeatedly before use. $(HF)_x$ was dried in a stainless steel bomb under 1.5 bar of F_2. CF_3NO was prepared according to the literature[11] and, after repeated distillation, stored in the dark in glass ampules. $N_2F^+AsF_6^-$ was prepared according to the literature[12] and stored under dry N_2.

[†] Universität Dortmund.

[‡] Universität-GH-Duisburg.

(1) Fox, W. B.; MacKenzie, J. S.; Vanderkooi, N.; Sukornick, B.; Wamser, C. A.; Holmes, J. R.; Eibeck, R. E.; Steward, B. B. *J. Am. Chem. Soc.* **1966**, *88*, 2604.

(2) Christe, K. O.; Maya, W. *Inorg. Chem.* **1969**, *8*, 1247.

(3) Dehnicke, K.; Aeissen, A.; Kölmel, M.; Strähle, J. *Angew. Chem.* **1977**, *89*, 569.

(4) Minkwitz, R.; Bernstein, D.; Sawodny, W.; Härtner, H. *Z. Anorg. Allg. Chem.* **1990**, *580*, 109.

(5) Christe, K. O.; Schack, C. J.; Wilson, R. D.; Pilipovich, D. *J. Fluorine Chem.* **1974**, *4*, 423.

(6) Ewig, C. S.; VanWazer, J. R. *J. Am. Chem. Soc.* **1990**, *112*, 109.

(7) Christe, K. O.; Wilson, W. W.; Schrobilgen, G. J.; Chirakal, R. V.; Olah, G. A. *Inorg. Chem.* **1988**, *27*, 789.

(8) Minkwitz, R.; Bernstein, D.; Sawodny, W. *Angew. Chem.* **1990**, *102*, 185. Minkwitz, R.; Bernstein, D.; Sawodny, W. *Angew. Chem., Int. Ed. Engl.* **1990**, *29*, 181.

(9) Fox, W. B.; Wamser, C. A.; Eibeck, R.; Huggins, D. K.; MacKenzie, J. S.; Juurik, R. *Inorg. Chem.* **1969**, *8*, 1247.

(10) Reed, A. E.; Schleyer, P. v. R. *J. Am. Chem. Soc.* **1990**, *112*, 1434.

(11) Umemoto, T.; Tsutsumi, H. *Bull. Chem. Soc. Jpn.* **1983**, *56*, 631.

(12) Moy, D.; Young, A. R., II. *J. Am. Chem. Soc.* **1965**, *87*, 1889.